Talanta 219 (2020) 121274

Contents lists available at ScienceDirect

Talanta

journal homepage: www.elsevier.com/locate/talanta

Double-site DNA walker based ternary electrochemiluminescent biosensor

Yue Huang[1], Xiaochun Zhu[1], Cenhong Jin, Weimin Li, Ying Zhou**, Ruo Yuan*

Chongqing Engineering Laboratory of Nanomaterials & Sensor Technologies, School of Chemistry and Chemical Engineering, Southwest University, Chongqing, 400715, PR China

ARTICLE INFO

Keywords:
Anatase TiO_2 nanocrystallines
Coreaction accelerator
Electrochemiluminescence
Double-site DNA walker

ABSTRACT

A novel biosensor was developed on the basis of Ru(dcbpy)$(bpy)_2^{2+}$/tripropylamine (TPrA)/TiO_2 nanocrystallines (TiO_2 NCs) as efficient electrochemiluminescence (ECL) ternary system and enzyme-driven double-site DNA walker as signal amplification strategy for the sensitive detection of carcinoembryonic antigen (CEA). Specifically, coreaction accelerator anatase TiO_2 NCs with catalytic activity could accelerate the oxidization of TPrA for prominently stimulating the ECL performance of Ru(dcbpy)$(bpy)_2^{2+}$/TPrA system to achieve the "signal on" state. Subsequently, numerous double-site walker DNA, converted from the target (CEA)-induced protein-aptamer cycle amplification, would trigger the detachment of Ru(dcbpy)$(bpy)_2^{2+}$ to reach the state of "signal-off". Benefiting from the above advantages, the developed ECL biosensor achieved outstanding sensitivity with a linear range from 500 pg/mL to 50 fg/mL and a detection limit down to 10.5 fg/mL. More importantly, the proposed strategy opens a new path for employing the ECL ternary system for sensitive detection of biomolecules and disease diagnosis.

1. Introduction

Electrochemiluminescence (ECL) has been widely identified to be a reliable analytical tool for the clinical detection of proteins, DNA, RNA and so on, owing to its fast analysis speed, outstanding controllability and good spatial resolution [4–6]. However, the traditional binary ECL system containing luminophore and coreactant was limited to further increase the ECL intensity, due to relatively low generation rate of reactive intermediates of coreactant around the electrode. In our previous work, some micromolecule or nanoparticle as the coreaction accelerator were introduced into binary systems to stimulate the oxidation or reduction rate of coreactant for notably amplifying the ECL signal of luminophore [7–9]. Since anatase TiO_2 nanocrystallines (TiO_2 NCs) contains abundant defects to produce plentiful oxygen vacancies for capturing electrons, thus presenting obvious catalytic activity. Above all, anatase TiO_2 NCs has employed as the coreaction accelerator of Ru(dcbpy)$(bpy)_2^{2+}$/tripropylamine (TPrA) system to construct a ternary ECL system, for significantly promoting the ECL signal of Ru(dcbpy)$(bpy)_2^{2+}$.

Recently, DNA nanomachines including DNA nanogears [10], DNA walkers [11], DNA tweezers [12] etc have paved a new approach to enrich the construction of biosensor. Particularly, DNA walkers showed up outstanding competence in the signal amplification and transduction in biological field due to its excellent flexibility, controllability, and locomotion. Regrettably, on account of the low binding efficiency, single-site walkers displayed inferior execution capacity for restricting the DNA amplification efficiency. More recently, the DNA walker with double binding site was put forward to replace the single-site walker [13,14], unfolding its merits of high binding efficiency and rapid movement. Herein, abundant double-site DNA walker was directly converted from target protein-induced protein-aptamer cycle amplification to trigger fast movement of DNA walker for realizing amplification of target.

Carcinoembryonic antigen (CEA) has been familiar as a common marker of breast cancer, lung cancer, colorectal cancer and other malignant tumors [1–3], therefore, the sensitive detection of CEA is of significant for clinic diagnosis and therapeutic evaluation of cancers. By using CEA as an analysis model, we reported the proof-of-concept of a sensitive and feasible ECL sensing platform for CEA detecting by combining Ru(dcbpy)$(bpy)_2^{2+}$/TPrA/TiO_2 NCs as high-efficient ECL ternary system and enzyme-driven double-site DNA walker as signal amplification strategy. As shown in Scheme 1A, in the presence of target CEA, the hairpin structure aptamer H_2 could be opened to form a CEA-aptamer binding complex (abbreviated as CEA@H_2) with an

* Corresponding author.
** Corresponding author.
E-mail addresses: zzying19@126.com, zzying19@email.swu.edu.cn (Y. Zhou), yuanruo@swu.edu.cn (R. Yuan).
[1] Author Contribution: Y. Huang and X.C. Zhu contributed equally.

https://doi.org/10.1016/j.talanta.2020.121274
Received 17 January 2020; Received in revised form 28 May 2020; Accepted 29 May 2020
Available online 08 July 2020
0039-9140/

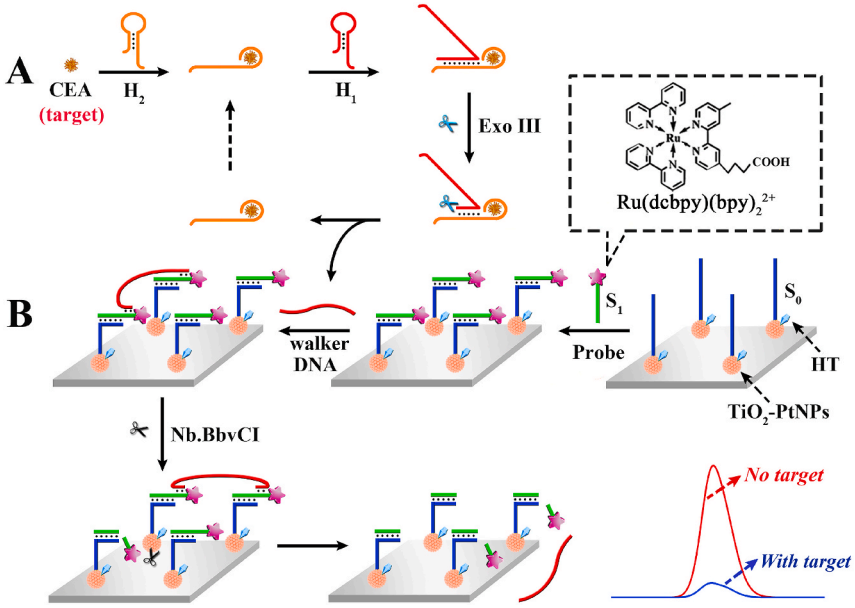

Scheme 1. (A) Exo III-assisted "protein-aptamer" cycle amplification strategy. (B) Fabrication of the ECL biosensor.

exposed DNA segment which further hybridized with H_1 to fabricate the complex structure CEA@H_1@H_2. Then enzyme EXO III was added to cleave the specific site of CEA@H_1@H_2 from the blunt end, resulting in the formation of secondary-target. From Scheme 1B, the DNA strand S_0 was immobilized on the TiO_2-PtNPs modified GCE interfacing *via* Pt–N bond. And then the DNA strand S_1 labeled with Ru(dcbpy)$(bpy)_2^{2+}$ was introduced to hybridize with S_0 to realize the close proximity between Ru(dcbpy)$(bpy)_2^{2+}$ and the coreaction accelerator TiO_2 NCs for obtaining strong ECL signal as the "signal-on" state. While the mixture of secondary-target and Nb.BbvCI enzyme was dropped in the surface of the modified GCE. Notably, secondary-target was designed as double-site DNA walker to hybridize with the exposed part of S_1 for triggering the Nb.BbvCI cleavage process. It accompanied by the detachment of Ru(dcbpy)$(bpy)_2^{2+}$ and DNA walker to manifest as a "signal off" state. Significantly, the novel coreaction accelerator was applied in the Ru complex/TPrA system to open a new insight for ternary ECL system in ultrasensitive biodetection.

2. Experiment section

2.1. Synthesis of TiO_2-PtNPs

Pt nanoparticles modified TiO_2 nanocrystallines (TiO_2-PtNPs) was prepared based on previous reports with the certain alteration [15,16]. Firstly, 3 mL isopropyl titanate was added to the solution containing 150 mL ethanol, 100 mL acetonitrile and 1.5 mL ammonium hydroxide and stirred for 6 h, then the suspension was centrifuged and washed thoroughly using absolute ethanol and distilled water two times to get pure TiO_2 NCs. Furthermore, 500 μL of 1% polyethyleneimine (PEI) was added to react with 1 mL of the obtained TiO_2 under stirring for 1 h. After the addition of $H_2PtCl_6{\cdot}6H_2O$ (500 μL, 1 mM), 100 μL freshly prepared ice cold $NaBH_4$ (1 mM) was dropwise mixed into the above solution and reacted under stirring for 1 h. Ultimately, after centrifugation and thorough clean with anhydrous ethanol and distilled water, the obtained TiO_2-PtNPs was dispersed into 1 mL of distilled water in an ultrasonic apparatus.

2.2. Synthesis of S_1–Ru(dcbpy)$(bpy)_2^{2+}$

Initially, 12 μL of Ru(dcbpy)$(bpy)_2^{2+}$ (80 μM) was added dropwise into the mixture consisting of 126 μL phosphate buffer solution (PBS), 50 mM N-Hydroxysuccinimide (NHS) and 200 mM N-(3-(dimethylamino) propyl)-N′-ethylcarbodiimide hydrochloride (EDC), then stirred for 120 min at 4 °C to activate its carboxyl. Secondly, 15 μL of NH_2-terminated single-stranded DNA S_1 (20 μM) was added to the solution mentioned above. Then the mixed solution was incubated for 4 h at 4 °C for the formation of the amino bond linking S_1–NH_2 and Ru(dcbpy)$(bpy)_2^{2+}$. Lastly, the prepared S_1–Ru(dcbpy)$(bpy)_2^{2+}$ was stored at 4 °C.

2.3. Exo III-Assisted "protein-aptamer" cycle

Firstly, H_1 and H_2 solution were severally heated to 95 °C for 2 min, followed by cooling off to 25 °C in 1 h to generate the hairpin structure. After that, 10 μL of CEA with various concentrations was added into 90 μL of mixture (1.0 μM hairpin-structured DNA H_1, 2.0 μM hairpin-structured DNA H_2, and 40 U of enzyme Exo III, respectively). Subsequently, the mixture was reacted for 75 min at 37 °C in a polymerase chain reaction (PCR) instrument to carry out the "protein-aptamer" cycle [17]. As shown in Scheme 1(A), after the target CEA with different concentrations was added to the solution containing H_1, H_2 and Exo III, the complex structure CEA@H_1@H_2 formed. Then Exo III cleaved specific site of CEA@H_1@H_2, resulting in the formation of double-site DNA walker with various concentrations, and the recycle CEA@H_2 complex also came into being simultaneously.

2.4. Fabrication of biosensor

In advance of modification, the glassy carbon electrode (GCE) (Φ = 4 mm) was polished with 0.3 and 0.05 μm alumina powder, following that the GCE was thoroughly cleaned by ultrasonic wave in anhydrous ethanol and distilled water in turn. The establishment of the biosensor is depicted in detail in Scheme 1(B). Initially, the polished GCE was covered by a droplet of 5.0 μL dispersed TiO_2-PtNPs owing to the excellent film formation capacity of TiO_2. Subsequently, 10 μL of amino-modified single-stranded DNA S_0 (1 μM) was immobilized on the TiO_2-PtNPs film through Pt–N bond after 16-h incubation at 4 °C.

After blocking with 1 mM hexanethiol (HT) for 2 h, 10 μL of prepared S_1–Ru(dcbpy)$(bpy)_2^{2+}$ was immobilized on the electrode through hybridizing with S_0 at 37 °C for 2 h, reaching the state of "signal-on". Subsequently, 20 μL of double-site DNA walker with different concentrations from "protein-aptamer" cycle was mixed with 20

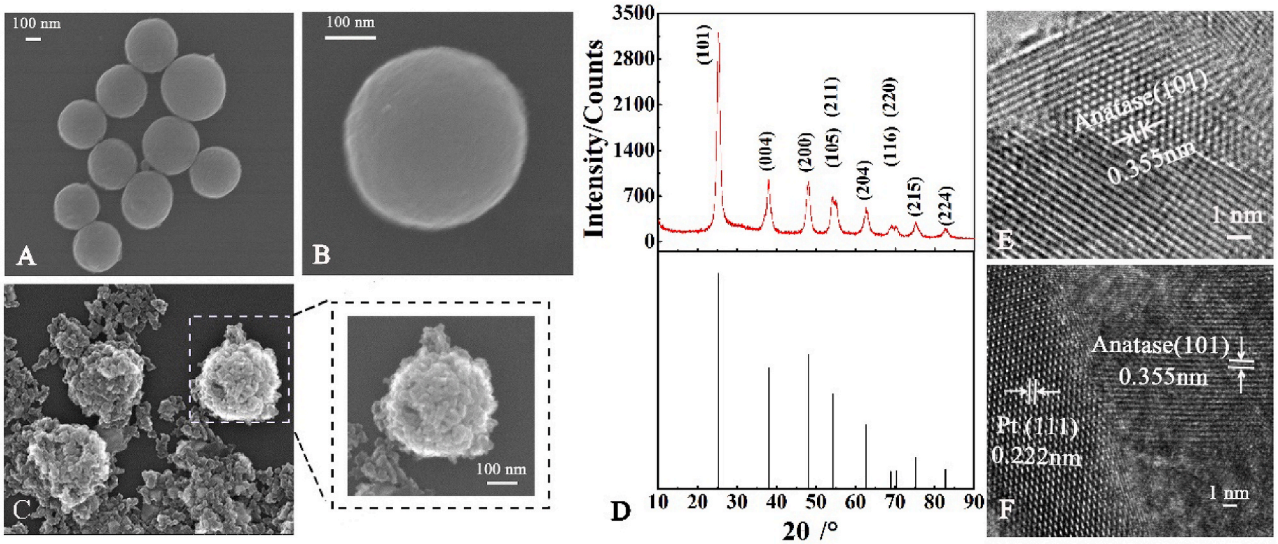

Fig. 1. SEM images of (A) TiO_2 NCs, (B) single TiO_2 NCs, (C) TiO_2-PtNPs and the insets of panels C is the amplified SEM image of TiO_2-PtNPs. (D) XRD pattern of obtained TiO_2 NCs (upper plot) compared to a standard PDF Card No. 65–5714 (lower plot). HRTEM image of (E) obtained TiO_2 NCs and (F) TiO_2-PtNPs.

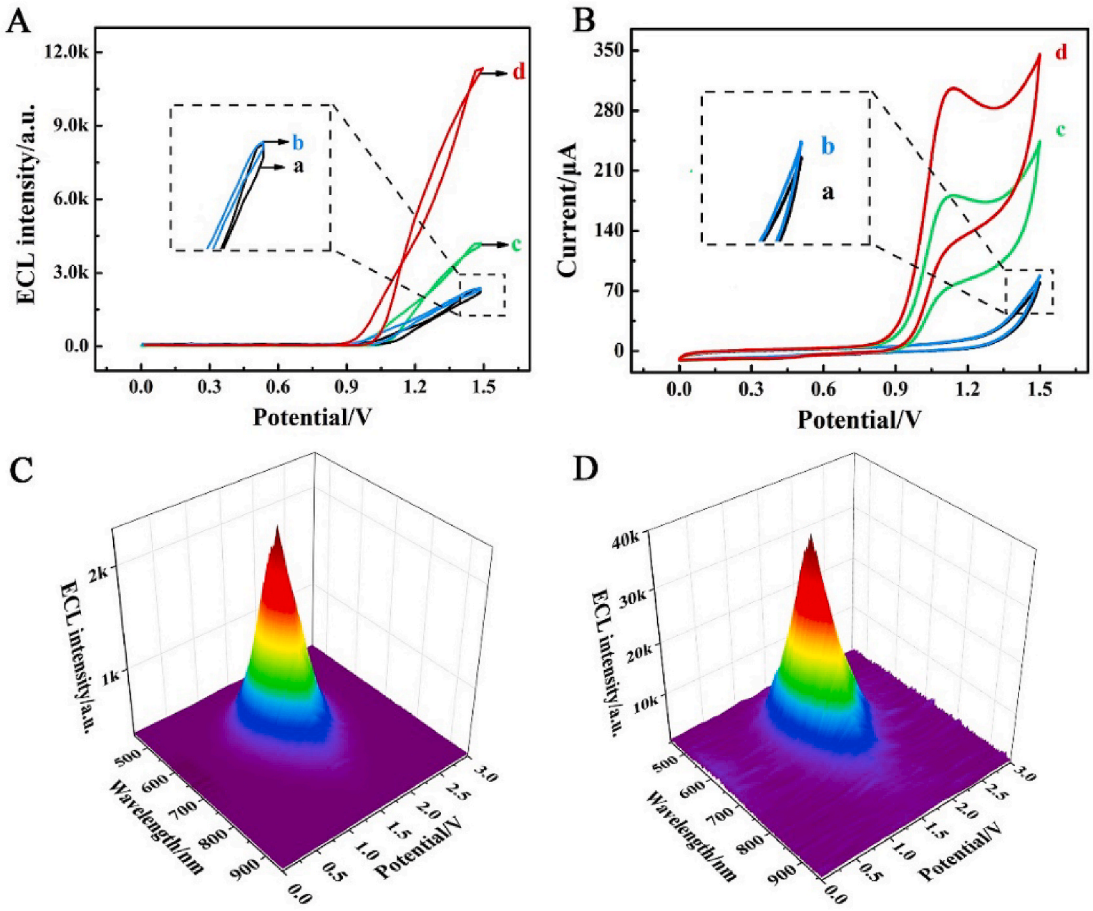

Fig. 2. The ECL responses (A) and CVs (B) of bare GCE (curve a) and TiO_2 NCs/GCE (curve b) in Ru(dcbpy)$(bpy)_2^{2+}$ solution, bare GCE (curve c) and TiO_2 NCs/GCE (curve d) in Ru(dcbpy)$(bpy)_2^{2+}$ + TPrA solution. The 3D surface image model of TiO_2 NCs/GCE in Ru(dcbpy)$(bpy)_2^{2+}$ solution (C) and Ru(dcbpy)$(bpy)_2^{2+}$ + TPrA solution (D). The concentration of Ru(dcbpy)$(bpy)_2^{2+}$ and TPrA was 0.1 μM and 1 mM, respectively.

U of Nb.BbvCI, respectively. Finally, 10 μL of the mixture was dropwise added to the electrode and incubated for 40 min to trigger the "signal-off" state. Finally, the prepared biosensor was stored at 4 °C to keep active and stable.

2.5. Measurement procedure

After rinsed by PBS (pH 7.4, 0.1 M), the ECL response measurement of the obtained biosensor was carried out in 3 mL PBS with TPrA (1 mM). The potential was set from 0 to 1.5 V at the scan rate of

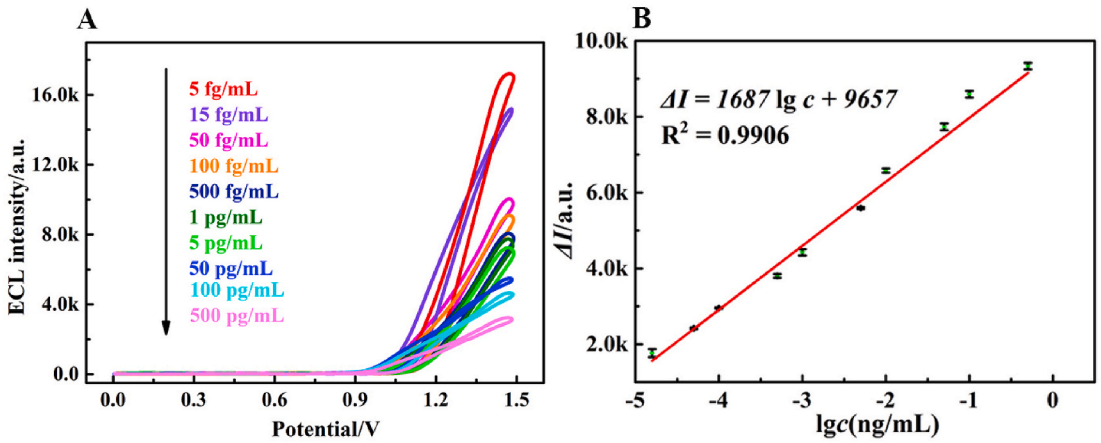

Fig. 3. (A) ECL profiles of the "signal-off" state in the presence of different concentrations of CEA. The concentrations of CEA: 15 fg/mL, 50 fg/mL, 100 fg/mL, 500 fg/mL, 1 pg/mL, 5 pg/mL, 50 pg/mL, 100 pg/mL, 500 pg/mL. (B) Calibration curve of the proposed biosensor.

Table 1
Comparison of analytical performance of different CEA detection assays.

Detection method	Linear range	LOD	Ref
Fluorescence	0.03 ng/mL ~6 ng/mL	7.9 pg/mL	[22]
UV–vis	0.2 ng/mL ~ 2.5 ng/mL	0.03 ng/mL	[23]
Photoelectrochemistry	5 ng/mL ~ 10 ng/mL	4.8 pg/mL	[24]
Electrochemistry	1 pg/mL ~ 0.1 μg/mL	0.1 pg/mL	[25]
ECL	5 pg/mL ~ 500 ng/mL	1.67 pg/mL	[26]
Electrochemistry	0.05 ng/mL ~ 100 ng/mL	21.1 pg/mL	[27]
ECL	50 fg/mL ~ 500 pg/mL	10.4 fg/mL	this work

300 mV/s with a high voltage of the photomultiple tube (PMT) at 800 V.

3. Results and discussion

3.1. Characterization of TiO_2-PtNPs

The morphologies of nanoparticles were characterized by scanning electron microscope (SEM) at a voltage of 15–20 kV. Fig. 1A and B were the SEM images of TiO_2 NCs and single TiO_2 nanocrystalline, displaying uniform and smooth spherical structures with an average size of 3.5 μm. When PtNPs were embedded into TiO_2 NCs, as Fig. 1C exhibited, it was obvious that abundant small particles were thick distributed on the surface of sphere, illustrating that PtNPs were successfully immobilized on TiO_2 NCs.Whereafter, Fig. 1D showed the X-ray diffraction (XRD) pattern of obtained TiO_2 NCs, in which the peaks were in conformity with the standard anatase TiO_2 NCs from PDF card No. 65–5714. In Fig. 1E and F, the lattice constant was examined to be 0.355 nm and 0.355 nm respectively, coinciding to the lattice fringes of anatase (101) plane [15]. Meanwhile, Fig. 1F displayed clear lattice fringes of TiO_2-PtNPs, where the interplanar spacing of 0.222 nm corresponded to the face-centered cubic (fcc) lattice of PtNPs nanocrystalline [18].

3.2. Electrochemical and optical properties of the system

To explore the enhancement mechanism of $Ru(dcbpy)(bpy)_2^{2+}$/TPrA/TiO_2 NCs system, the ECL responses and corresponding CV responses of bare GCE and GCE modified with TiO_2 NCs (TiO_2 NCs/GCE) were investigated. From Fig. 2A, the ECL intensities of bare GCE (curve a) and TiO_2 NCs/GCE (curve b) in PBS with 0.1 μM $Ru(dcbpy)(bpy)_2^{2+}$ were observed to be roughly the same and inferior, manifesting that TiO_2 NCs has no direct enhancement on the ECL performance of luminophore $Ru(dcbpy)(bpy)_2^{2+}$ in absence of coreactant. When coreactant TPrA (1 mM) was added, the ECL responses of bare GCE (curve c) and TiO_2 NCs/GCE (curve d) increased to 4030.3 a.u and 11282 a.u, respectively. According to the above results and previous related literature [19,20] of metal nanoparticles as coreactant accelerator, it could be speculated that TiO_2 NCs could act as coreaction accelerator in

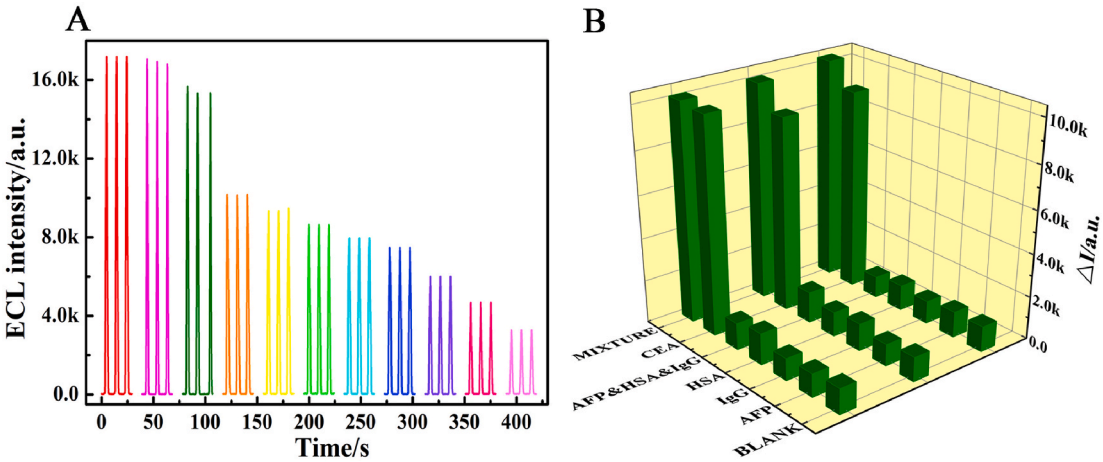

Fig. 4. (A) Stability of the prepared biosensor under the state of "signal-on" (red curve) and various concentrations of CEA: 50 fg/mL, 100 fg/mL, 500 fg/mL, 1 pg/mL, 5 pg/mL, 50 pg/mL, 100 pg/mL, 500 pg/mL. (B) Selectivity of the biosensor with 500 pg/mL CEA against interference proteins: AFP, IgG and HSA. (For interpretation of the references to color in this figure legend, the reader is referred to the Web version of this article.)

$Ru(dcbpy)(bpy)_2^{2+}$/TPrA system. Therefore, the cyclic voltammetry (CV) characterization was researched to further investigate the speculation. As can be seen Fig. 2B, both peak current and peak potential of bare GCE (curve a) and TiO_2 NCs/GCE (curve b) in $Ru(dcbpy)(bpy)_2^{2+}$ solution remained basically consistent. When TPrA was introduced into the detection solution, the peak current of bare GCE (curve c) significantly increased, while a new oxidation peak displayed at about 1.13 V, implying that TPrA was oxidized during this process. Furthermore, TiO_2 NCs/GCE was immersed in $Ru(dcbpy)(bpy)_2^{2+}$ + TPrA solution, the peak current (curve d) was distinctly stronger than that of bare GCE (curve c) whereas peak potential stayed unchanged. It could indicate that TiO_2 NCs indeed acted as coreactant accelerator to facilitate the oxidation of TPrA for generating more oxidizing intermediate, enhancing ECL emission of $Ru(dcbpy)(bpy)_2^{2+}$. Besides, the 3D surface image of bare GCE and TiO_2 NCs/GCE in $Ru(dcbpy)(bpy)_2^{2+}$ + TPrA solution were characterized. Fig. 2C showed that the maximum ECL emission of bare GCE in PBS containing $Ru(dcbpy)(bpy)_2^{2+}$ + TPrA exactly corresponded to the previous report [21], with a location at 628 nm. Moreover, when TiO_2 NCs/GCE was detected in above base solution, the maximum ECL wavelength (Fig. 2D) appeared the same wavelength, but the maximum ECL emission was great stronger than that of GCE. These results showed that TiO_2 NCs is a highly efficient coreactant accelerator in $Ru(dcbpy)(bpy)_2^{2+}$/TPrA system.

The possible ECL mechanism was described in the following equations:

$$Ru(dcbpy)(bpy)_2^{2+} - e^- \rightarrow Ru(dcbpy)(bpy)_2^{3+} \quad (1)$$

$$TPrA - e^- \rightarrow TPrA^{\bullet +} \quad (2)$$

$$TPrA^{\bullet +} \rightarrow TPrA^{\bullet} + H^+ \quad (3)$$

$$Ru(dcbpy)(bpy)_2^{3+} + TPrA^{\bullet} \rightarrow Ru(dcbpy)(bpy)_2^{2+*} \quad (4)$$

$$Ru(dcbpy)(bpy)_2^{2+*} \rightarrow Ru(dcbpy)(bpy)_2^{2+} + h\nu \quad (5)$$

3.3. Performance of the ECL biosensor toward CEA

3.3.1. Calibration trace

The sensitivity of the CEA detection biosensor was evaluated after incubating with the mixture of Nb.BbvCI and the released DNA walker with various concentrations under the optimal experimental conditions. Firstly, as shown in Fig. 3A, the ECL response descended in turn along with the concentration of CEA ascended. Moreover, as displayed in Fig. 3B, an outstanding linear relationship between the decline of ECL responses and the logarithm values of the CEA concentration was obtained. The linear equation was fitted to be $\Delta I = 1687 \lg c + 9657$ with the correlation coefficient square of 0.9906, where c represented the concentration of CEA. Additionally, the limit of detection (LOD) was calculated to be 10.4 fg/mL (the calculation process in detail was placed in the Supporting Information), and compared with previous reports (Table 1), the elaborated biosensor performed better in the linear range and LOD, which manifested it has great potentiality in the clinical bioassay field.

3.3.2. Stability and selectivity of the ECL biosensor

Stability, selectivity and reproducibility are crucial factors to evaluate performance of the proposed biosensor. To estimate the stability, the ECL responses of biosensors incubated with various CEA concentrations under continuous cyclic scans were recorded. As depicted in Fig. 4A, the ECL response curves remained stable for 3 cycles and scarce variation could be observed, indicating an excellent stability of the biosensor. As shown in Fig. 4B, the selectivity of the proposed biosensor was further investigated by using three interference reagents alpha fetoprotein (AFP) (10 ng/mL), human immunoglobulin G (IgG) (10 ng/mL) and human serum albumin (HSA) (10 ng/mL) to perform contrastive experiments. As expected, a low ΔI was observed when CEA was replaced with alpha fetoprotein (AFP) (10 ng/mL), human immunoglobulin G (IgG) (10 ng/mL) and human serum albumin (HSA) (10 ng/mL), respectively, which showed little variations compared with blank experiment. Moreover, ΔI of the biosensor with the mixture of CEA (500 pg/mL), HSA (10 ng/mL), AFP (10 ng/mL) and IgG (10 ng/mL) turned out to be similar with that of the pure CEA (500 pg/mL). The results above verified that HSA, AFP, and IgG cannot cause interference to the proposed biosensor. In brief, contrast assay illustrated the biosensor exhibited an excellent selectivity of CEA.

4. Conclusion

In summary, a ECL biosensor was designed based on $Ru(dcbpy)(bpy)_2^{2+}$/TPrA/TiO_2 NCs as high-efficient ECL ternary system and double-site DNA walker as signal amplification for sensitive determination of CEA. Primarily, the anatase TiO_2 NCs was employed to facilitate the ECL emission of $Ru(dcbpy)(bpy)_2^{2+}$/TPrA binary system to construct the high-intense state of “signal-on”. Secondly, the DNA walker, was converted from a small number of target CEA through the protein-aptamer cycle, rapidly detached the luminophore $Ru(dcbpy)(bpy)_2^{2+}$ with the assistance of Nb.BbvCI, leading to the state of “signal-off”. As expected, the developed biosensor exhibited high sensitivity, wide linear range and excellent selectivity. Impressively, the proposed strategy opens up a new method for employing the ECL ternary system for detection and analysis of biomolecules.

Credit Author Statement

Yue Huang, Conceptualization; Data curation; Formal analysis; Investigation; Writing - original draft; Writing - review & editing, Xiaochun Zhu: Conceptualization; Data curation; Formal analysis; Investigation; Writing - original draft; Writing - review & editing. Cenhong Jin: Data curation; Investigation. Weimin Li: Conceptualization; Writing - original draft; Supervision. Ying Zhou: Resources; Project administration; Supervision. Ruo Yuan: Funding acquisition; Resources; Writing - review & editing.

Declaration of competing interest

The authors declare that they have no known competing financial interests or personal relationships that could have appeared to influence the work reported in this paper.

Acknowledgements

This work was financially supported by the NNSF of China (21775124, 21575116, 21675129), and the Fundamental Research Funds for the Central Universities (XDJK2018AA0003), China We also thanked Xia Zhong (Southwest University) for the electrochemical technical support.

Appendix A. Supplementary data

Supplementary data to this article can be found online at https://doi.org/10.1016/j.talanta.2020.121274.

References

[1] T. Kamisawa, Laura D. Wood, T. Itoi, K. Takaori, Pancreatic cancer, Lancet 10039 (2016) 73–85.
[2] Z.Y. Zhong, Y.G. Zhai, P. Bu, S. Shah, L. Qiao, Papilloma-pseudovirus eradicates intestinal tumours and triples the lifespan of $Apc^{Min/+}$ mice, Nat. Commun. 8 (2017) 15004.
[3] V.K. Singha, S. Kumarb, S.K. Pandeya, S. Srivastavab, M. Mishrac, G. Guptac, B.D. Malhotrab, R.S. Tiwaria, A. Srivastava, Fabrication of sensitive bioelectrode based on atomically thin CVD grown graphene for cancer biomarker detection, Biosens. Bioelectron. 105 (2018) 173–181.

[4] A.M. Zhang, C.C. Miao, H.Y. Shi, H.K. Xiang, C.S. Huang, N.Q. Jia, A novel solid-state electrochemiluminescence sensor for atropine determination based on Ru $(bpy)_3^{2+}$/carbon nanospheres/Nafion composite film, Biosens. Bioelectron. 122 (2018) 231–238.
[5] D.T. Tran, V.H. Hoa, L.H. Tuan, N.H. Kim, J.H. Lee, Peptide cleavage induced assembly enables highly sensitive electrochemiluminescence detection of protease activity, Biosens. Bioelectron. 119 (2018) 134–140.
[6] Z.Y. Liu, W.J. Qi, G.B. Xu, Recent advances in electrochemiluminescence, Chem. Soc. Rev. 44 (2015) 3117–3142.
[7] Y. Zhou, M.X. Chen, Y. Zhuo, Y.Q. Chai, W.J. Xu, R. Yuan, In situ electrodeposited synthesis of electrochemiluminescent Ag nanoclusters as signal probe for ultrasensitive detection of cyclinD1 from cancer cells, Anal. Chem. 89 (2017) 6787–6793.
[8] Y.M. Lei, R.X. Wen, J. Zhou, Y.Q. Chai, R. Yuan, Y. Zhuo, Silver ions as novel coreaction accelerator for remarkably enhanced electrochemiluminescence in a PTCA−$S_2O_8^{2-}$ system and its application in an ultrasensitive assay for mercury ions, Anal. Chem. 90 (2018) 6851–6858.
[9] S.S. Yang, M.H. Jiang, Y.Q. Chai, R. Yuan, Y. Zhuo, Application of antibody-powered triplex-DNA nanomachine to electrochemiluminescence biosensor for the detection of anti-digoxigenin with improved sensitivity versus cycling strand displacement reaction, ACS Appl. Mater. Interfaces 10 (2018) 38648–38655.
[10] D.F. Feng, X.C. Tan, Y.Y. Wu, C.H. Ai, Y.N. Luo, Q.Y. Chen, H.Y. Han, Electrochemiluminecence nanogears aptasensor based on MIL-53(Fe)@CdS for multiplexed detection of kanamycin and neomycin, Biosens. Bioelectron. 129 (2019) 100–106.
[11] W. Engelen, S.P.W. Wijnands, M. Merkx, Accelerating DNA-Based computing on a supramolecular polymer, J. Am. Chem. Soc. 140 (2018) 9758–9767.
[12] P. Zhang, J. Jiang, R. Yuan, Y. Zhuo, Y.Q. Chai, Highly ordered and field-free 3D DNA nanostructure: the next generation of DNA nanomachine for rapid single-step sensing, J. Am. Chem. Soc. 140 (2018) 9361–9364.
[13] T.E. Tomov, R. Tsukanov, Y. Glick, Y. Berger, M. Liber, D. Avrahami, D. Gerber, E. Nir, DNA bipedal motor achieves a large number of steps due to operation using microfluidics-based interface, ACS Nano 11 (2017) 4002–4008.
[14] F. Fakhari, S.E. Rokita, A walk along DNA using bipedal migration of a dynamic and covalent crosslinker, Nat. Commun. 5 (2014) 5591.
[15] J.H. Pan, X.Z. Wang, Q.Z. Huang, C. Shen, Z.Y. Koh, Q. Wang, A. Engel, D.W. Bahnemann, Large-scale synthesis of urchin-like mesoporous TiO_2 hollow spheres by targeted etching and their photoelectrochemical properties, Adv. Funct. Mater. 24 (2014) 95–104.
[16] M. Paszkiewicz, J. Łuczak, W. Lisowski, P. Patyk, A. Zaleska-Medynska, The ILs-assisted solvothermal synthesis of TiO_2 spheres: the effect of ionic liquids on morphology and photoactivity of TiO_2, Appl. Catal., B 184 (2016) 223–237.
[17] M.Q. He, K. Wang, W.J. Wang, Y.L. Yu, J.H. Wang, Smart DNA machine for carcinoembryonic antigen detection by exonuclease III-assisted target recycling and DNA walker cascade amplification, Anal. Chem. 89 (2017) 9292–9298.
[18] W.Y. Gao, M.Q. Wang, C.X. Ran, X. Yao, H.H. Yang, J. Liu, D.L. He, J.B. Bai, One-pot synthesis of Ag/r-GO/TiO_2 nanocomposites with high solar absorption and enhanced anti-recombination in photocatalytic applications, Nanoscale 6 (2014) 5498–5508.
[19] J.L. Liu, Z.L. Tang, Y. Zhuo, Y.Q. Chai, R. Yuan, Ternary electrochemiluminescence system based on Rubrene microrods as luminophore and Pt nanomaterials as coreaction accelerator for ultrasensitive detection of MicroRNA from cancer cells, Anal. Chem. 89 (2017) 9108–9115.
[20] F.F. Wu, Y. Zhou, H. Zhang, R. Yuan, Y.Q. Chai, Electrochemiluminescence peptide-based biosensor with heteronanostructures as coreaction accelerator for the ultrasensitive determination of tryptase, Anal. Chem. 90 (2018) 2263–2270.
[21] J.L. Liu, M. Zhao, Y. Zhuo, Y.Q. Chai, R. Yuan, Highly efficient intramolecular electrochemiluminescence energy transfer for ultrasensitive bioanalysis of aflatoxin M1, Chem. Eur J. 23 (2017) 1853–1859.
[22] Y.J. Wang, Z.K. Wei, X.D. Luo, Q. Wan, R.L. Qiu, S.Z. Wang, An ultrasensitive homogeneous aptasensor for carcinoembryonic antigen based on upconversion fluorescence resonance energy transfer, Talanta 195 (2019) 33–39.
[23] X. Wang, B. Zhang, J. Li, H.H. Chang, W.L. Wei, A simple and fast chromogenic reaction based on Ag_3PO_4/Ag nanocomposite for tumor marker detection, Talanta 175 (2017) 229–234.
[24] Z.L. Qiu, J. Shu, J.F. Liu, D.P. Tang, Dual-channel photoelectrochemical ratiometric aptasensor with up-converting nanocrystals using spatial-resolved technique on homemade 3D printed device, Anal. Chem. 91 (2019) 1260–1268.
[25] M.R. Akanda, H.X. Ju, A tyrosinase-responsive nonenzymatic redox cycling for amplified electrochemical immunosensing of protein, Anal. Chem. 88 (2016) 9856–9861.
[26] N.L. Liu, L.P. Jia, R.N. Ma, W.L. Jia, Y.Y. Lu, S.S. Shi, H.S. Wang, A novel sandwiched electrochemiluminescence immunosensor for the detection of carcinoembryonic antigen based on carbon quantum dots and signal amplification, Biosens. Bioelectron. 89 (2017) 453–460.
[27] S.X. Wu, H.L. Tan, C. H Wang, J.H. Wang, S.R. Sheng, A colorimetric immunoassay based on coordination polymer composite for the detection of carcinoembryonic antigen, ACS Appl. Mater. Interfaces 11 (2019) 43031–43038.